

UNCLASSIFIED

AD . 413922

DEFENSE DOCUMENTATION CENTER

FOR

SCIENTIFIC AND TECHNICAL INFORMATION

CAMERON STATION, ALEXANDRIA, VIRGINIA



UNCLASSIFIED

NOTICE: When government or other drawings, specifications or other data are used for any purpose other than in connection with a definitely related government procurement operation, the U. S. Government thereby incurs no responsibility, nor any obligation whatsoever; and the fact that the Government may have formulated, furnished, or in any way supplied the said drawings, specifications, or other data is not to be regarded by implication or otherwise as in any manner licensing the holder or any other person or corporation, or conveying any rights or permission to manufacture, use or sell any patented invention that may in any way be related thereto.

CATALOGED BY DDC
AS AD No. 413922

ASD-TDR-63-184

DEVELOPMENT PROGRAM FOR AN INERTIAL SENSOR TECHNIQUE

TECHNICAL DOCUMENTARY REPORT ASD-TDR-63-184

JUNE 1963

AF FLIGHT DYNAMICS LABORATORY
AERONAUTICAL SYSTEMS DIVISION
AIR FORCE SYSTEMS COMMAND
WRIGHT-PATTERSON AIR FORCE BASE, OHIO

Project No. 8222, Task No. 82209

Prepared under Contract No. AF 33(616)-7756
by
SPERRY GYROSCOPE COMPANY
Division of Sperry Rand Corporation
Great Neck, New York

413922

NO ORS



NOTICES

When Government drawings, specifications, or other data are used for any purpose other than in connection with a definitely related Government procurement operation, the United States Government thereby incurs no responsibility nor any obligation whatsoever; and the fact that the Government may have formulated, furnished, or in any way supplied the said drawings, specifications, or other data, is not to be regarded by implication or otherwise as in any manner licensing the holder or any other person or corporation, or conveying any rights or permission to manufacture, use, or sell any patented invention that may in any way be related thereto.

ASTIA release to OTS not authorized.

Qualified requesters may obtain copies of this report from the Armed Services Technical Information Agency, (ASTIA), Arlington Hall Station, Arlington 12, Virginia.

Copies of this report should not be returned to the Aeronautical Systems Division unless return is required by security considerations, contractual obligations, or notice on a specific document.

This report has been prepared by the Sperry Gyroscope Company Division of Sperry Rand Corporation, Great Neck, New York, on Air Force contract AF33(616)7756, under Task No. 822209 of Project No. 8222, "Development Program for an Inertial Sensor Technique". The work was administered under the direction of Flight Control Technology Laboratory,* Aeronautical Systems Division. Mr. Anthony De Thomas was project engineer for the Laboratory.

The studies presented began in February 1961, were concluded in December 1962, and represent the effort of the Air Armament Division of the Sperry Gyroscope Company under the direction of Division Scientist Willis G. Wing.

This report is the final report and concludes the work on contract AF33(616)7756. The contractor's report number is CA-4211-0158.

*Presently designated Flight Control Division of AF Flight Dynamics Laboratory.

This program demonstrated the feasibility of a new gyroscope technique for sensing inertially derived control data. This technique measures centrifugal pressures at the surface of a spinning fluid sphere. These pressures represent displacement of the container axis from that of the fluid and are converted to electrical signals by microphones. The two gyroscope models which were built demonstrated low random drift ($0.02^\circ/\text{hr}$), large linear range ($<0.1^\circ/\text{hour}$ to $5^\circ/\text{second}$ with 2% accuracy), short warm-up time (less than 2 minutes), and design simplicity. They are two-axis gyroscopes.


The main problem encountered was sensitivity to cross spin axis linear acceleration which, theoretically, can cause apparent drift if axial thermal gradient is present. The design of the models guarded against inducing thermal gradients but neglected to consider the pressures which could be produced in the fluid by the expansion bellows. This design oversight caused large g-sensitive errors but tests were arranged to observe this error with the bellows caged. The error then was less than $5^\circ/\text{hr/g}$.

In its present state of development this gyroscope is particularly adaptable to strapped down applications where high rates must be accepted without sacrificing low rate performance.

PUBLICATION REVIEW

This technical documentary report has been reviewed and is approved.

FOR THE COMMANDER


H. W. BASHAM
Actg Chief
Flight Control Division

<u>Section</u>		<u>Page</u>
I	INTRODUCTION	1-1
II	DESIGN DISCUSSION	2-1
	2-1. Phase I Feasibility Studies	2-1
	2-2. Phase II Gyroscope Models	2-10
III	TEST PROCEDURES AND RESULTS	3-1
	3-1. Test Procedures	3-1
	3-2. Discussion of Model I Test Results	3-2
	3-3. Discussion of Model II Test Results	3-4
	3-4. Additional Performance Data	3-5
IV	CONCLUSIONS	4-1
<u>Appendix</u>		
A	ILLUSTRATIONS	A-1

<u>Figure</u>		<u>Page</u>
2-1	Gyroscope Time Constant vs Spin Speed	A-2
2-2	Fluid Sphere Reaction to Applied Torques	A-3
2-3	Transducer Back Passages	A-4
2-4	Fluid Sphere Back-Passage Arrangement for Second-Harmonic Angular-Vibration Degeneration	A-5
2-5	Inductive Slip Ring Signal Coupler	A-6
2-6	Cutaway View of Gyroscope	A-7
2-7	Test Circuit - Fluid Sphere Gyroscope	A-8
2-8	Detail Photographs	A-9
3-1	Sensitivity and Drift - Model I	A-10
3-2	Noise - Model I	A-10
3-3	Linear Acceleration Sensitivity - Model I	A-10
3-4	Linear Acceleration Sensitivity - Model II	A-11
3-5	Sensitivity and Drift - Model II	A-11
3-6	Noise - Model II	A-11
3-7	Typical Test Set-Up	A-12

SECTION I
INTRODUCTION

The ultimate aim of this program has been to advance the state of the art of instrumentation by demonstrating the feasibility of a new gyroscope technique for sensing inertially derived control data. The work on this program was performed by the Sperry Gyroscope Company Division of Sperry Rand Corporation, Great Neck, New York, under Contract AF33(616)7756 for the Aeronautical Systems Division, Air Force Systems Command, Wright-Patterson Air Force Base, Ohio.

The technique used is that of measuring centrifugal pressures at the surface of a spinning fluid sphere, the sphere having a spin axis parallel to its container except when an angular rate is applied to the container about any normal to its spin axis. When this input rate is applied, a relative displacement between the container and fluid axes occurs. Port holes, for sensing pressure, are placed 45 degrees from the cavity axis and sense sinusoidally varying pressure at the spin frequency when the axes are displaced. The ports connect to microphones which convert the pressure to electrical signal. The magnitude of the pressure is proportional to the input rate; the phase defines the input axis. The instrument becomes a two-axis device when the total signal is demodulated with respect to a zero- and a 90-degree rotor position reference.

Manuscript released by Sperry Gyroscope Company April 1963
for publication as an ASD Technical Documentary Report.

The transfer function, volts out per angle in, for each axis is

$$\frac{e}{\theta} = \frac{K\tau}{\tau s + 1}$$

where

K = sensitivity constant,

τ = characteristic time associated with axis
realignment, and

s = complex operator.

The program comprised two phases. Phase I of the program was devoted to the investigation and study of a new inertial technique, and to the design of a fluid sphere gyroscope with its various elements to implement this technique. The details of the work performed in Phase I have already been presented in an Interim Technical Report, dated November 1961, and entitled Development Program for an Inertial Sensor Technique.

This Final Technical Report reviews the Phase I effort and presents the work accomplished in Phase II of the program. This second phase has been devoted to the construction and test of the fluid sphere gyroscope envisioned in the design study of Phase I. The results of this work prove, not just the feasibility, but the realization of a new sensing technique which will ultimately permit sensor designs of greater simplicity, reliability, accuracy, and life span with reduced size, weight, power consumption, and cost.

Two models of the new gyroscope have been fabricated and tested. Both models (with overall dimensions of 2 1/4-inch diameter and 8 1/4-inch length) have 1.5-inch fluid-sphere sensitive elements. Each weighs 5 pounds and uses 22 watts, 10 volts, 200 cps for its motor drive. The signal source requires 27 volts dc at 40 ma. Each gyroscope has an input and an output transformer. The input impedance is 1600 ohms at 41 kc, and the output impedance is 10K ohms, inductive. The test results achieved on these models have demonstrated that the fluid-sphere device is presently suited to sensitive rate measurements, high-acuity dynamic angular measurements, and inertial stabilization - all with a short warm-up time.

The Model I performance data which follow were taken after only one minute of gyroscope warm-up.

- Output two axes
- Angular rate threshold 0.2°/hr
- Random drift (rms excursion from mean,
for one hour) 0.2°/hr
- Random noise (6-cps bandwidth) 0.3°/hr
- Sensitivity to linear acceleration
(in the plane normal to the spin axis - zero
for accelerations along the spin axis) 4°/hr/g

Model II performance data were taken at a temperature selected to give solid fluid fill, as explained in the text. It was tested at high rates to find the points where axis definition and linearity degenerate.

• Angular rate threshold	0.1°/hr
• Random drift (rms excursions from mean, 3 hours)	0.04°/hr
• Noise (20-cps bandwidth) total	0.3°/hr
• Sensitivity to linear acceleration	3°/hr/g
• Dynamic range	180,000:1
Linearity	<3% f.s. to 5°/sec
Cross coupling	<2° axis shift to 1°/sec.

There is evidence that the sensitivity to linear acceleration is not a functional limitation of the device, but a design problem specific to these models.

Along with study of the gyroscope itself there have been related investigations of devices for coupling electrical information from rotating to non-rotating members. A capacitive gear tooth chopper was unsuccessful. A rotary transformer proved practical and was used for both signal and excitation coupling. A mercury grounding element has proven very reliable.

In addition to the test performance data, there are a number of other pertinent features worthy of comment:

- a) No temperature control is used.
- b) There is no mechanical upper limit on rate range (sensitive element is displaced only 1° at an 11°/sec input rate).

- c) No malfunctions have occurred in either unit (one has operated 400 hours).
- d) Performance does not deteriorate with age.

It is evident that this gyroscope can provide advantages over all other types of comparable accuracy both in low cost of manufacture and in long life with high reliability. Low cost because of absence of critical manufacturing tolerances; long life and high reliability because of the reduction to one moving part, which rotates at moderate speed on bearings which can be moderately loaded and amply lubricated; and because reasonable dimensional changes have no influence on drift performance. Those dimensional changes which produce shift of the center of gravity relative to the center of support in the wheel gyroscopes do not affect the fluid rotor which has an inherently coincident center of gravity and center of buoyancy. Such changes which cause change of static capacitance balance in the microphones have only a second order effect, since only their response to spin frequency pressures is of interest.

SECTION II

DESIGN DISCUSSION

2-1. PHASE I FEASIBILITY STUDIES

A. Summary

A number of valuable conclusions were derived from the laboratory investigations and theoretical studies conducted during Phase I; these data, in turn, influenced the design of various elements of the gyroscope.

The study performed in Phase I of the program began with some knowledge of fluid sphere behavior. It had been demonstrated that, while developed signal pressure increased as the square of spin speed, the time constant decreased seemingly in a linear manner with spin speed. Also, that transducer and passage impedances were functions of spin speed. Experiment had shown that the time constant could not be shortened as much as one part in thirty by sphere prolateness nor could it be significantly increased by lapping the sphere surfaces to a high polish.

Another study investigated the relationship between gyroscope time constant and spin speed. The results are shown in figure 2-1. The calculated line is at 3 db per octave. Observed data departs from this line in a manner consistent with a coriolis degenerative influence. Since a long time constant is desirable in the fluid sphere, gyroscope spin speed has been reduced from 12,000 rpm, as originally planned, to 6000 rpm.

The study of time constant vs speed was made with a laboratory model, designed originally with a 3-inch sphere and a spin speed of 6000 rpm. Single-axis responses to

angular step functions, observed at various speeds, are plotted in figure 2-1. Uncertainty in the measurements is evident in the spread of plotted points. A calculated point, P, is shown and based on the expression

$$\tau = \frac{R}{5} \sqrt{\frac{2}{\nu \omega}}$$

where

τ = time constant,

R = sphere radius,

ν = kinematic viscosity, and

ω = spin angular velocity.

To derive this expression, the sphere is considered a solid body with a shearing layer at the boundary; the thickness of this layer being taken as the distance from the boundary to the radius at which the decay of induced oscillatory motion is 63 percent. The above expression predicts the 3 db per octave decay with speed, as shown. The experimental data, however, show a tendency toward 6 db per octave. This tendency is due probably to additional degeneration from coriolis effects. An attempt has been made to obtain more experimental knowledge of coriolis effects by inducing flow into the model sphere; however, it is evident that the deterioration of the time constant at 12,000 rpm is so great that a lower speed must be used. The 6000 rpm is chosen somewhat arbitrarily. Meanwhile, a study has been made of flow effects in the sphere and back passages. The results appear below.

Transducer port and passage impedances affect fluid sphere behavior, since coriolis torques result from

fluid signal drain. The various effects on sphere position and signal pressure are discussed below, with the justification for using intersecting back passages, one with, and one without, transducers.

Signal coupling from rotating to non-rotating members will be accomplished with a rotating transformer. Use of a capacitive gear tooth coupling was investigated, but the results were unsatisfactory.

B. Transducer Port Design

The study phase of the program has shed some light on factors influencing transducer port design. The sphere time constant decreases with speed at a rate between 3 and 6 db per octave. This is due to two effects: viscous shear of the fluid, and coriolis degeneration. The former effect, due to sphere wall drag, is believed to be a torque which produces a restoring rotation about the input axis and also a component about the axis normal to both the input and spin axes. The shear effect must be tolerated, except for its normal component. It may be possible to cancel this normal component by a component of the coriolis effect. The coriolis torque results from the draining of fluid from the sphere in the process of signal generation and is dependent on the back passage impedance. For resistive (dissipative) impedance in the back passages, the coriolis torque exerted on the sphere is degenerative; for conservative impedances, a cross coupling effect is produced. Consider a fluid sphere with the input rotation shown in figure 2-2. The flow along path a, b, c is not constrained and exerts on the sphere a side force F , a torque T , and an angular rotation ω_D , ($\vec{T} = \vec{\omega}_D \times \vec{H}$), for dissipative back passage impedance ($\Delta P/\dot{q}$). For inductive flow ($\Delta P/\dot{q}$ proportional to spin speed), the force, torque,

and angular rotation lag by 90 degrees of spin rotation. The effect is to drive the sphere axis in the ω_I direction. This causes an output about the axis normal to the original input, that is, cross coupling. There is no accurate quantitative knowledge of the above effects.

Flow in the back passages is more controllable, and something is known about its behavior. When passages intersect, there is coriolis coupling between them. The effect of this coupling is reinforcing if the source passage has an inductive (mass effect) impedance.

All these factors must be taken into account in the design of the ports and passages. One other consideration is second-harmonic angular vibration, a noise source which produces a spin frequency output from the transducers and is distinguishable from the signal only because it has the opposite phase rotation. This fact causes an inductive passage to couple degenerative coriolis pressure and, consequently, to oppose flow due to this source. Use is made of this characteristic in the design of the fluid sphere gyroscope.

Figure 2-3 shows the cross section of (a) the active, or signal producing port and passage, and (b) the coriolis assisting passage. The latter, containing no transducers, is a highly inductive impedance. The signal pressure flow in this passage aids signal flow in the active passage; the effect of second-harmonic angular-vibration-generated flow opposes the same effect in the active passage. This is independent of the impedance of the active passage.

A comparison of the effects of shear-torque cross coupling and coriolis cross coupling leads to the conclusion that these effects are opposing (for inductive back passages) and tend to cancel each other. This is desirable.

As figure 2-2 shows, with a developed shear torque, \underline{T} , in the $\Delta\omega$ direction, the sphere reaction is $\underline{\omega}_M$ due to its angular momentum \bar{H} , and $\bar{\omega}'_I$ due to its moment of inertia. The latter reaction is a cross coupling effect and is opposite in sense to the $\bar{\omega}_I$, noted above, for the case of coriolis torque for inductive back passages.

C. Determination of Port and Passage Impedance

Port impedance is arbitrarily designed to attempt cancellation of the cross coupling components of shear and coriolis torques.

The shear torque component can be estimated from the time-constant measurements, using the expressions for time constant (τ), shear torque (T_S) and developed signal pressure (P).

$$\tau = \frac{R}{5} \sqrt{\frac{2}{\nu \omega}}$$

$$T_S = \frac{d}{\tau} H$$

where

d = angular offset between case and sphere,

H = fluid sphere angular momentum,

and

$$P = \rho \omega^2 R^2 d.$$

The shear torque in terms of signal pressure, then, is

$$T_S = \frac{PH}{\rho \omega^2 R^2 \tau}$$

The signal pressure causes back passage flow in the relationship

$$PA = \rho \ell_b A \omega^2 dx$$

where

A = area of back passage,

ℓ_b = length of back passage, and

dx = amplitude of fluid linear displacement.

The coriolis force F in the sphere is

$$F = \rho \ell_s A 2 \omega^2 dx$$

where

ℓ_s = length of path in sphere (= $\sqrt{2}$ R), and

A is assumed to be the same as for the back passage.

The coriolis torque is $R/\sqrt{2}$ times this force

$$T_C = 2 \rho A R^2 \omega^2 dx = \frac{2PAR^2}{\ell_b} .$$

Setting $T_C = T_S$

$$\frac{2PAR^2}{\ell_b} = \frac{PH}{\rho \omega^2 R^2 \tau} .$$

The angular momentum H is

$$H = \frac{8}{15} \pi \rho R^5 \omega .$$

Solving for the back passage dimension relationship

$$\frac{A}{\ell_b} = \frac{4 \pi R}{15 \tau \omega} .$$

Using the experimental value of τ , and correcting for the radius difference between the laboratory model and the new gyroscope

$$\frac{A}{l_b} = \frac{4\pi (3/4) (2.5^4)}{15 (628) (0.15)} = 0.017 \text{ cm.}$$

Assuming the effective back passage length for both passages is 4 cm

$$A = \frac{\pi D^2}{4} = (4) (0.017)$$

and

$$D = 0.3 \text{ cm} = \text{diameter of back passages.}$$

D. Impedance of the Active Passage

The impedance, defined as pressure per quantity flow rate, is calculated in dyne seconds per cm^5 . The inductive component is a function mainly of passage configuration, the resistive is primarily the damping in the transducer gap, and the capacitive is the diaphragm spring. Predicted values are

$$Z_I = \frac{\Delta P_I}{\dot{q}} = \frac{\omega \rho l}{A} = \frac{(1.8) (628) (2)}{(0.12)} = 19 \times 10^3$$

$$Z_R = \frac{\Delta P_R}{\dot{q}} = \frac{\mu l D^3}{A^2 g^3} = \frac{(1.8) (10^{-2}) (38) (0.038)^3}{(5)^2 (10^{-2}) (0.005)^3} = 1.2 \times 10^3$$

where

μ = absolute viscosity,

l = length of stator lands,

D = width of stator lands,

A = diaphragm area under stator, and

g = gap.

$$Z_C = \frac{\Delta P_C}{\dot{q}} = \frac{1.7 Et^3}{\omega(1 - \nu^2) r^6} + \frac{1.4 St}{\omega r^4} = 5000 + 4500 = 9.5 \times 10^3$$

where

E = Young's modulus,

t = diaphragm thickness,

ν = Poisson's ratio,

r = diaphragm radius, and

S = stress.

The natural frequency of the active passage is somewhat lower than the 6000-rpm spin speed, and the passage impedance is largely inductive.

E. Design of the Assisting Passage

This back passage is used to provide cancellation of second harmonic angular vibration by coriolis coupling to the active passage. In figure 2-4, the assisting passage (X) is used to develop a coriolis pressure P_Y equal to the source pressure P_X . Cancellation is then effected.

$$A_Y P_Y = ma = m 2 \omega v = \rho A_X l_X 2 \omega^2 dx$$

where

a = coriolis acceleration, and

dx = amplitude of fluid linear displacement.

Since this passage is designed to be essentially inductive, the source pressure (appearing at the active and assisting ports in time quadrature) is related to the flow in passage (X) as

$$P_X = \rho \ell'_X \omega^2 dx$$

where

ℓ'_X = effective total passage length.

The condition for cancellation then is

$$\frac{\ell'_X}{\ell_X} = 2 \frac{A_X}{A_Y}.$$

F. Signal Coupling

Conventional slip rings are unreliable at speeds being considered in this program. An effort was made to develop a capacitive gear tooth coupler to take information off the rotating member. The function of the coupler was to couple an electrical signal and chop it at a frequency equal to the number of teeth times spin speed. Results were not satisfactory and the effort has been abandoned. Specifically, the capacitance variation in the model was too small in the presence of average value plus stray capacitance (an rms value of 1 to 2 pf in the presence of 100 pf).

The coupling chosen as satisfying design requirements is similar to that which couples power to the rotating members, and consists simply in a ferrite-core rotating transformer with axial windings in both rotor and stator. (See figure 2-5.) The air gap is 0.002 inch. This device, designed for use at about 45 kc, presents a low Q-tuned impedance to the transducer. Measurements of gain (output voltage per transducer capacity change) indicated 500 mv/pf per volt excitation to be a reasonable design goal.

2-2. PHASE II GYROSCOPE MODELS

This description of the fluid sphere gyroscope can best be followed by referring to the cutaway drawing of the model shown in figure 2-6. The discussion is based on the elements of the gyroscope - going from the basic to the peripheral. Emphasis is placed on those features where most of the work was done.

The 1.5-inch diameter sphere (1) is filled with a fluorochemical FC75 (3M designation). This fluid has a density of 1.76 gm/cc, a kinematic viscosity of 0.8 at 25°C, a dielectric constant of 1.85, a reasonable vapor pressure, and compatibility with other materials. It is desirably close in density to magnesium, making the transducer elements essentially floated. The sphere develops a signal pressure of about 10 dynes per square centimeter per arc second of case spin axis displacement from fluid sphere spin axis. The case spin axis is (2) and the input axes of the gyro are shown as (3). Since viscous shear and coriolis degeneration tend continually to coerce the axes of sphere and case into alignment, there is a time constant involved. This, with the displacement sensitivity, yields

a rate sensitivity; pressure per input rate is equal to pressure per displacement times time constant. One aim to the program was to maximize this rate sensitivity.

As discussed at some length in the interim report, this maximization is not simply a matter of using a high spin speed. Time constant decreases with spin speed at something between 3 and 6 db/octave and transducer-passage hydraulic impedances are functions of spin speed. It was found that the best response could be obtained at about 6000 rpm where measured time constant was 0.09 second.

The problem of isolating the fluid sphere from mechanical distortions of the case and from axial thermal gradients was solved effectively by containing the inner member (4) (sphere plus transducers) in fluid and supporting its ends within the case by radially stiff webs (5). The webs decouple case distortions from the inner member and thermal isolation is improved by the fluid surrounding the inner member.

Expansion bellows (7) are placed at each end of the sealed rotating case (6). An attempt was made to isolate any vibratory effects they might send toward the transducers. These bellows are gas filled with a bias pressure of 50-psi gauge so there will be no void when the device is spun at low temperature. The bellows are caged; as the gyro temperature rises they lift off their stops and obtain some limited radial freedom. It is believed that the failure to contain these bellows radially has contributed significantly to the gyroscope's linear acceleration sensitivity, but just how this occurs is not known. It is known that the dynamic balance of the rotating member is affected as the bellows get off their stops. It

is also known that the linear acceleration sensitivity rises markedly at the same time. It is possible that the change in sensitivity arises from fluid coupling of pressure from bellows to transducer, and is quite separate from the change in balance, though both have the same source.

The transducer element, a capacitive microphone, is made of magnesium (which has the same density as the fluid) and is thus insensitive to accelerations. The transducer diaphragm (8) is of 0.002-inch stretched foil and the stator (9), displaced 0.002-inch from it, is a grid to allow fluid flow. The static capacity of the device is 25 pf. Used in pairs, the diaphragms are excited by opposite-phase, equal-amplitude, 41-kc carrier. The stators are electrically connected. Differential fluid signal pressures exerted on the diaphragms, produce a signal at the stators which is coupled to the non-rotating member of a rotary transformer (10). A second rotary transformer (11) of the same mechanical design is used to couple the carrier aboard.

These coupling devices were used because they do not have the wear problems of conventional slip rings and were found to be functionally adequate. Both rotor and stator have axial windings set into ferrite cores. The magnetic circuit around the windings is completed through a small (0.002 - to 0.003-inch) radial gap (12). Both rotor and stator are potted assemblies with steel mounting rings.

Considerable care was exercised in the radial positioning of the rotary transformers. Lack of concentricity of rotor and stator and spin axis could cause a variation of effective gap and a consequent change of the transformer inductance, which could result in modulation of the transmitted carrier and apparent output.

The rotating member was grounded without conventional slip rings. A hollow torus containing mercury was mounted at one end of the rotating assembly and contact was made with the stator through a stainless steel disc. This device has operated without leak or malfunction for over 400 hours on the first model.

As a rotary-position reference for demodulation of the signal and definition of the input axes, a simple alternator (13) was used. This was the stator of a size 10 synchro resolver and a diameter-magnetized, permanent-magnet rotor. The resulting spin-frequency sine waves on the stator windings were in phase quadrature. There were some problems with this unit. The wave shape was not symmetrical and the duty cycle of the demodulator was affected directly. Variation in duty cycle would appear as rotation of the gyroscope drift vector, so an attempt was made to eliminate this source. Reduction of the rotor diameter did not appreciably improve the wave shape and filtering made the gyroscope somewhat sensitive to motor speed fluctuations, the phase shift in the filter appearing as output noise at motor hunt frequencies. Testing was done, therefore, with no filter and with recognition that the reference was less than ideal.

The four-pole, hysteresis, synchronous motors (14) operate from a single-phase, 8- to 15-volt supply with a phase-splitting capacitor. If connected in series, their voltage requirement is doubled. In the test program the ability to vary drive speed was desired, so motors were operated from an oscillator and power amplifier. The test results were taken with 8-volt, 200-cps excitation which gave a motor speed of 6000 rpm.

The external electronics used are shown schematically in figure 2-7. The circuit is straightforward. The signal exists at the gyroscope output as spin frequency modulation of the residual carrier (this residual carrier is the electrical unbalance of the transducer circuit). After some amplification, full wave detection produces the signal at spin frequency. This is fed to a ring demodulator using one of the alternator outputs as reference. The demodulator output is a direct voltage measure of the input rate about one of the axes, defined by the reference generator.

Filters in the circuit are used to reject the second harmonic of the carrier after detection, and to reject the second harmonic of spin frequency after demodulation. In the test circuitry a low-pass filter was used at the drift recorder and a band-pass (0.02 to 6 cps) electronic filter defined the band for noise measurements.

Photographs of individual details are shown in the montage of figure 2-8.

SECTION III
TEST PROCEDURES AND RESULTS

3-1. TEST PROCEDURES

Two types of tests were performed to determine the capabilities of the gyroscopes. In each of these, the motor speed was controlled at 6000 rpm, the speed determined to give the optimum time constant of 0.09 second. Details of the two tests are given below. The details of the circuit are given in figure 2-7.

Test 1

Drift, Sensitivity, and Noise

Conditions

Spin axis vertical

Seismically quiet mount

Operation from a cold start

Rotation about spin axis at one revolution each twelve minutes.

These conditions were chosen for several reasons. The spin axis being vertical eliminates acceleration sensitivities which are to be examined separately. The verticality of the spin axis and slow rotation about it allows convenient calibration. The quiet mount keeps out ambient floor disturbances.

Measurements

Sensitivity - response to $\pm 11.3^\circ/\text{hr}$ (horizontal component of earth rate)

Drift - total drift from turn-on, each axis

- rms excursion from mean for first hour

Noise - amplitude and frequency content in pass-band 0.02 cps to 6 cps

Test 2

Linear Acceleration Sensitivity

Conditions

Same as Test 1, except spin axis aligned to earth's polar axis and

- a) Gyro run cold (75° to 85°F)
- b) Gyro run warm (approximately 115°F)

Measurements

Two axis output vs position in the gravity field

3-2. DISCUSSION OF MODEL I TEST RESULTS

The sensitivity and drift, noise, and linear acceleration sensitivity curves are shown in figures 3-1, 3-2, and 3-3, respectively.

While the measured sensitivity and drift speak for themselves, it should be noted that most of the "noise" present is not random noise. The 1-cps and 2-cps components each have sources which will yield to study and be eliminated. They do not hamper use of the gyroscope as a gyro compass, of course, even if not eliminated.

The main problem in overall performance is the linear acceleration sensitivity. It was noted that there was a marked change between operation at 80°F and at 120°F. At the higher temperatures there is a g-sensitivity of 110°/hr/g, while there is only about 4°/hr/g with the gyroscope cool. It is believed that this is a gravity-sensitive fluid pressure at spin frequency within the gyroscope which appears as the gyroscope becomes warm. Such a vibration

could be caused by the bellows. The two bellows, one at each end of the rotating member; are pressure loaded at 50-psi gauge and axially caged at 75°F. As the fluid expands in heating, the bellows are lifted off their stops separately at between 85°F and 95°F. To the extent that the uncaged bellows are buoyant and can respond at 100 cps, they are signal-frequency pressure sources in the fluid. To the extent that these pressures can reach the transducers as differential pressures, gravity-sensitive output is produced. Although there is considerable baffling between bellows and transducer, it is not isolation.

The one known theoretical source of linear acceleration sensitivity is axial thermal gradient. This causes fluid density to vary axially and appears as a mass unbalance. It is possible that the 4°/hr/g is wholly or partly attributable to this, but rotor temperatures could not be measured well enough to determine this. It was, however, verified by temperature observations through the case, that axial thermal gradient was not related to the 110°/hr sensitivity. This sensitivity was related to average rotor temperature as stated previously.

Model I Test Results

Test 1

Sensitivity - 2 millivolts 1°/hr at demodulator output

Drift - (degrees per hour)

Motor on at 8:56	Time	Axis A	Axis B
	9:00	0	0
	9:20	-0.2	-0.1
	9:40	-0.3	-0.2
	10:00	-0.4	-0.3
	11:00	-0.7	-0.4 (°/hr)

-rms excursion from mean for first hour; readings every 100 seconds - $0.2^{\circ}/\text{hr}$

Noise - $1^{\circ}/\text{hr}$ peak-to-peak, at 1 cps
- $1^{\circ}/\text{hr}$ peak-to-peak, at 2 cps, phase rotation of 2 cps with respect to 1 cps at one cycle per 30 seconds

Test 2

Linear acceleration sensitivity

- Gyro cold $4^{\circ}/\text{hr}/\text{g}$
- Gyro hot $110^{\circ}/\text{hr}/\text{g}$

3-3. DISCUSSION OF MODEL II TEST RESULTS

Model II was filled at an elevated temperature (95°F) so that the linear acceleration performance could be observed as the device warmed up and passed through three modes of operation: first, with a bubble in the fluid, then no bubble and bellows seated and, last, bellows lifted by fluid expansion. It was hoped that the second condition could be held with enough stability to get a good reading of the linear acceleration sensitivity minimum with neither bellows nor bubbles interfering.

After some observations at various motor power levels, one was chosen which seemed to settle near the desired temperature. A plot of the resulting linear acceleration response is shown in figure 3-4.

For this test the spin axis is aligned to the polar axis and the input axes are exposed to $\pm 0.759 \text{ g}$ as the table rotates about the spin axis at one revolution per twelve minutes (the conditions of Test 2 above). As the gyro temperature arrives at the condition of no bubble and bellows still seated the g-sensitive excursions reduce to 5 chart divisions peak-to-peak, that is, $3^{\circ}/\text{hr}/\text{g}$.

Drift of this gyro was measured only after the temperature was high enough to assure a solid fluid fill (Test 1 above). Consequently it does not illustrate the short ready time of the first model. Its drift and noise levels, however, are better than for Model I. This is attributed to the intersecting passage transducer scheme described in Section II. A two-hour drift trace, figure 3-5, has an rms excursion from mean drift of less than $0.04^\circ/\text{hr}$. Readings were taken every 100 seconds. The noise, figure 3-6, in a 20-cps bandwidth, is $1^\circ/\text{hr}$ peak-to-peak, mostly 3 cps with some higher frequency content at about 6 cps.

3-4. ADDITIONAL PERFORMANCE DATA

This gyroscope has been operated on a temporary mount for five days (11/12 through 11/16/62), twelve hours a day, for observation by people in the industry and the services. Operating conditions were those of Test 1: spin axis vertical and the output of one axis recorded. A periodic exposure of this input axis to the earth rate horizontal component provided a chart calibration. The performance record is on two pieces of chart paper, one for the first four days, one for the fifth. These are available but not easily included in this report. From time to time the gyroscope was allowed to drift with its azimuth position undisturbed from one to three hours. Although there were sporadic angular deflections of the mount for demonstrations during these periods, the results were reasonable and are listed below, the data taken as before.

<u>Date</u>	<u>Time</u>	<u>Random Drift</u>
11/13/62	4 1/2 hours	0.069°/hr
11/14/62	2 1/2 hours	0.072°/hr
11/14/62	2 1/2 hours	0.071°/hr
11/16/62	5 hours	0.233°/hr

Figure 3-7 shows a typical test set-up which is available for further demonstrations.

SECTION IV

CONCLUSIONS

These fluid sphere gyroscope models have demonstrated remarkable reliability, range, and sensitivity with low random drift and short ready time. Neither malfunctions nor performance deterioration has occurred in over 400 hours of operation of each gyroscope.

The dominant performance problem is sensitivity to cross-spin-axis linear acceleration. This problem lies in expansion compensation of these particular models and is not a basic problem of the sensor technique. The three to four degrees per hour per g in these gyroscopes should be reducible by more than an order of magnitude in any subsequent design.

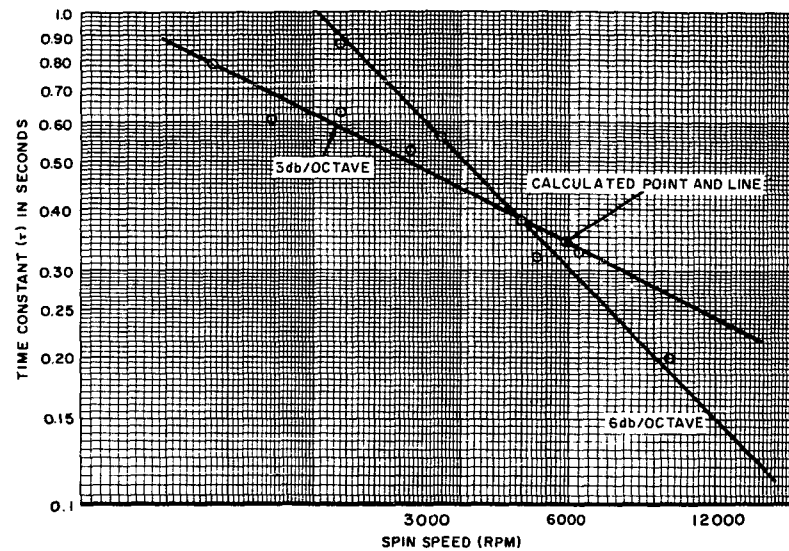
Applications for the fluid sphere gyroscope extend from inertial stabilization to rate measurements of many degrees per second. The instruments are particularly adaptable to strapped down applications because they have extremely high range and are inherently free from hysteresis. Measurements of the very low rates are unaffected by high rates in the recent past. Also, no danger of damage from input rate overloading exists. The ability to measure angular rates from well below 0.1 degree per hour to 5 degrees per second is more than 200,000:1 and can be translated according to the needs of application.

The dimensions of the study models were larger than those anticipated for production gyroscopes. It is believed that the same exhibited performance can be duplicated in a size having a 2-inch diameter and a 4.5-inch

length, including an electronic package which would supply signal excitation, amplification, and demodulation. The production gyroscope would use a 5-watt synchronous motor and weigh 2-1/2 pounds. The instruments would be more insensitive to linear accelerations and the operating range could be adjusted upward by using a fluid with higher viscosity.

APPENDIX A

This appendix contains all the illustrations referenced in this report. The illustrations are numbered in accordance with the section to which they apply, the first Arabic number indicating the section followed by a dash and Arabic numeral which indicates the illustration sequence in the section. The illustrations bear page numbers. The alphabet letter indicates the appendix to which the illustrations apply followed by a dash and Arabic number which indicates the illustration sequence in that appendix.



CALCULATED TIME CONSTANT
FROM SHEAR CONSIDERATIONS

$$\tau = \frac{R}{5} \sqrt{\frac{2}{\nu \omega}}$$

R = SPHERE RADIUS
 ν = FLUID KINEMATIC VISCOSITY
 ω = SPIN SPEED

NOTE:
 CALCULATIONS BASED ON
 3-IN.- DIAMETER LABORATORY
 MODEL FLUID SPHERE GYROSCOPE.

FIGURE 2-1. GYROSCOPE TIME CONSTANT VS SPIN SPEED

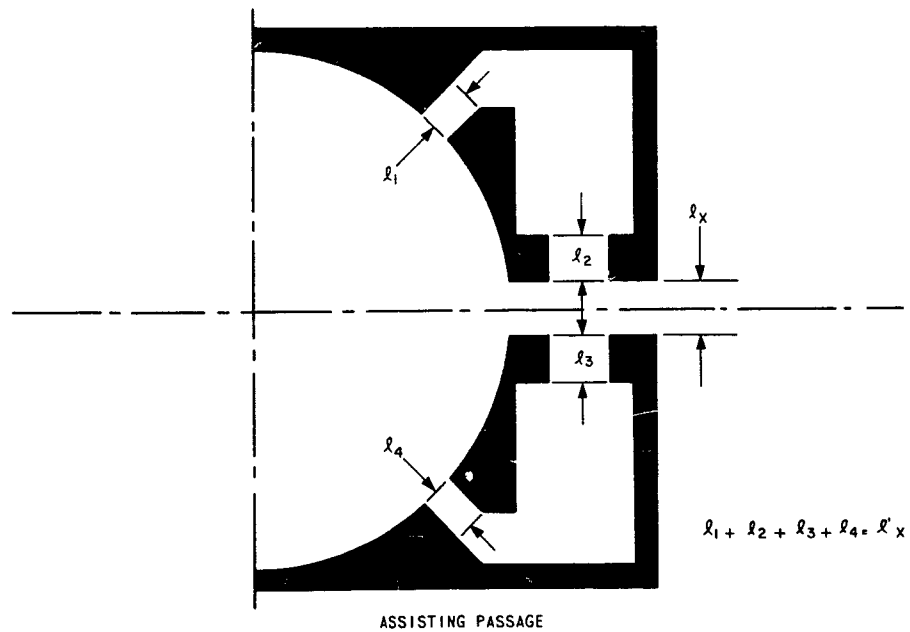
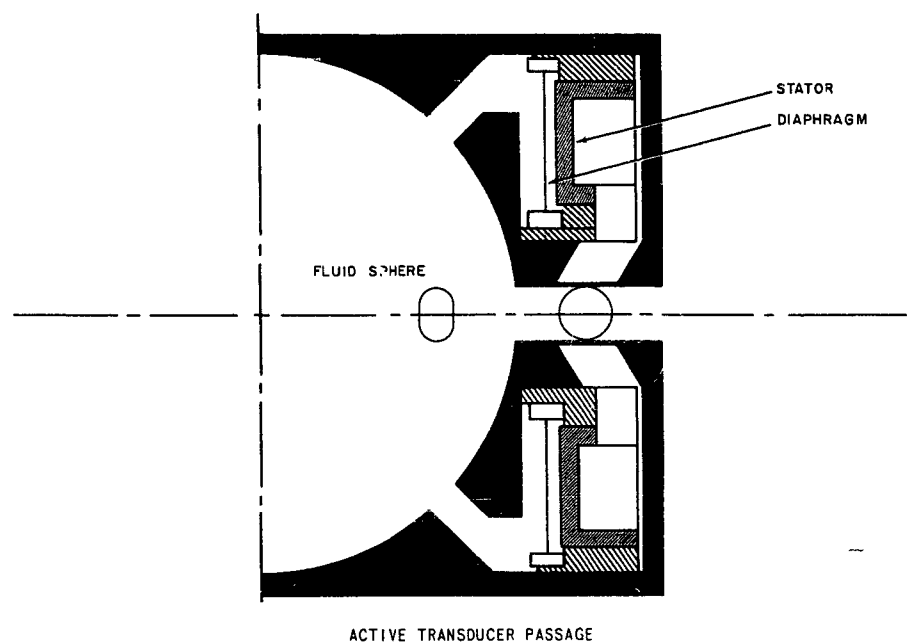


FIGURE 2-3. TRANSDUCER BACK PASSAGES

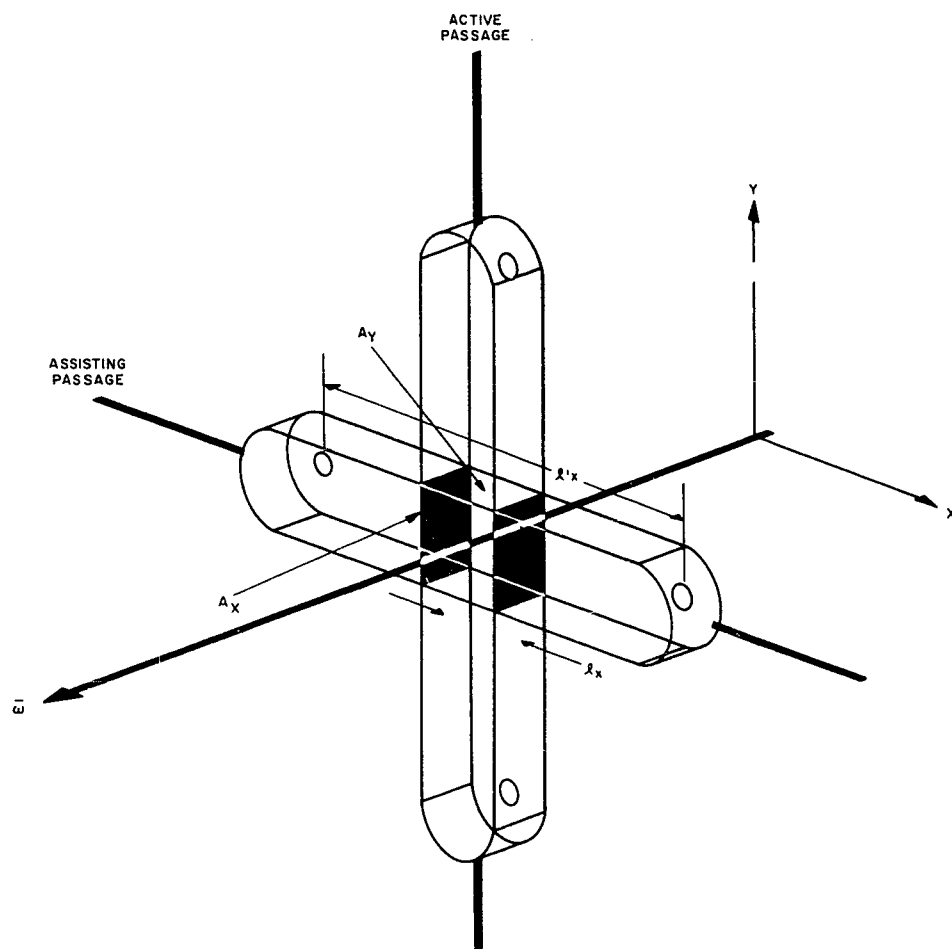


FIGURE 2-4. FLUID SPHERE BACK-PASSAGE ARRANGEMENT FOR SECOND-HARMONIC ANGULAR-VIBRATION DEGENERATION

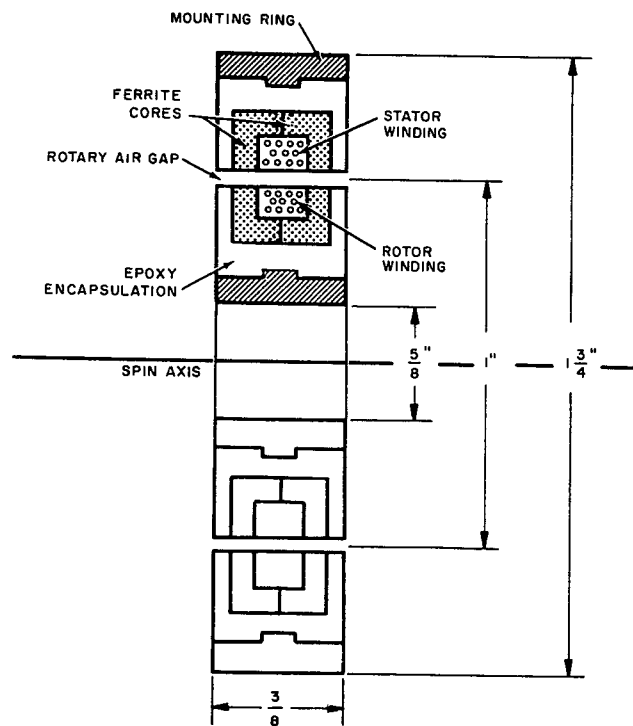


FIGURE 2-5. INDUCTIVE SLIP RING SIGNAL COUPLER

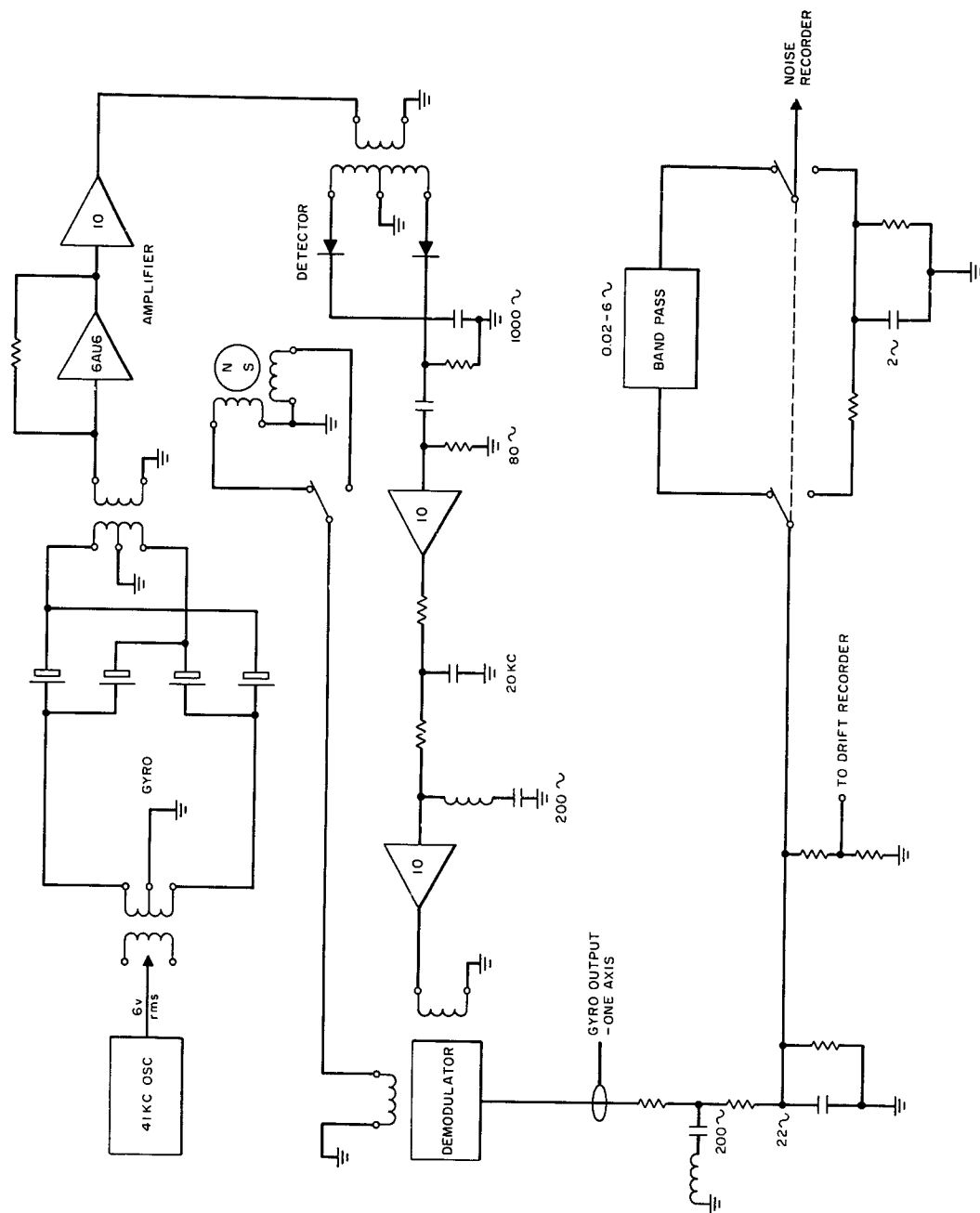
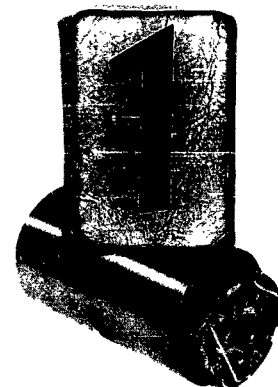


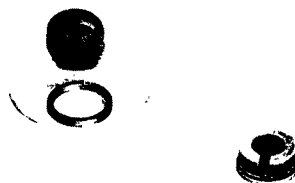
FIGURE 2-7. TEST CIRCUIT - FLUID SPHERE GYROSCOPE



Hemispheres showing transducer sockets



Inner Member, well
rotating case



Transducer

Left: stator, diaphragm ring and
stretched magnesium drumhead

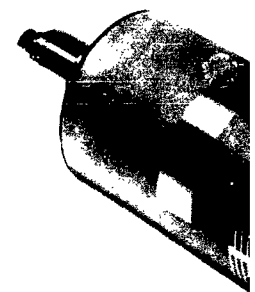
Right: assembly, diaphragm untrimmed



Rotating Assembly -
from end of shaft
ring, motor hyst
shielded rotary
electrical term

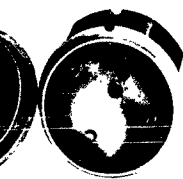


Inner Member assembled and wired - left
and right ends

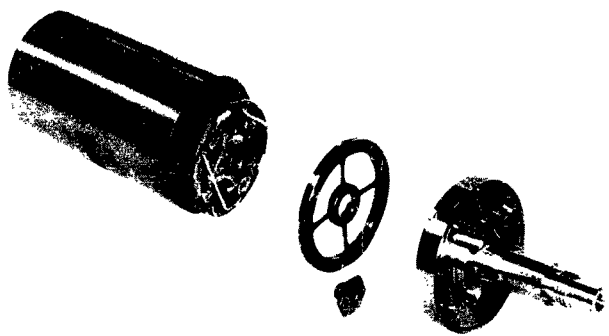


Rotating Assembly -
from end of shaft
ring, motor hyst
shielded rotary
electrical term

2



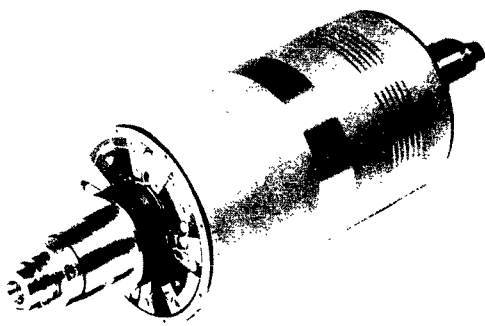
sockets



Inner Member, web suspension, locknut, rotating case, and shaft



and
unhead
ntrimmed



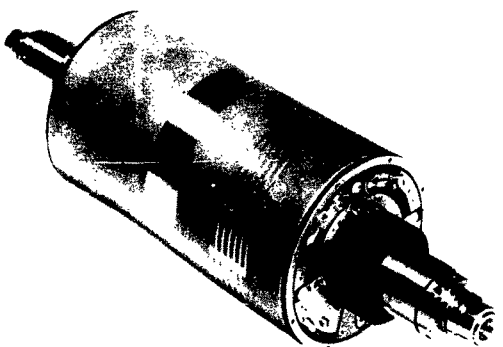
Rotating Assembly - Signal End, showing, from end of shaft, bearing race, lock ring, motor hysteresis ring, spacer, shielded rotary transformer rotor, electrical terminals



End housings, ou



- left



Rotating Assembly - Excitation End, showing, from end of shaft, bearing race, lock ring, motor hysteresis ring, spacer, shielded rotary transformer rotor, electrical terminals

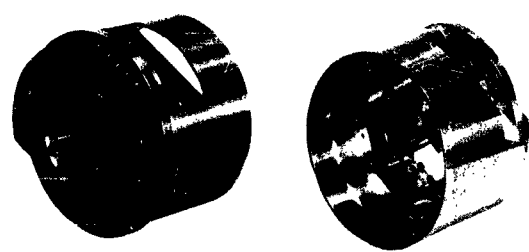


Assemb

3



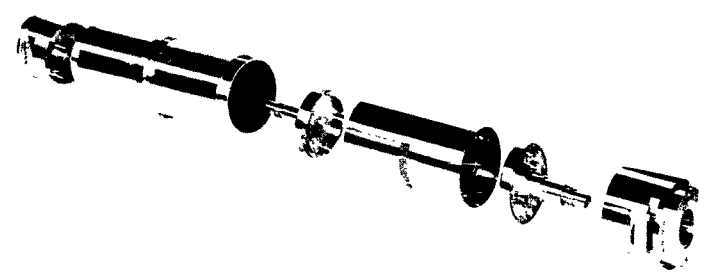
locknut,



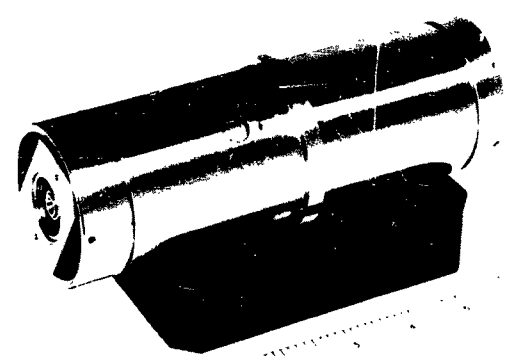
End housings



showing,
race, lock
, spacer,
rotor,



End housings, outer case, rotating case and shafts



Assembly - End Assemblies Off



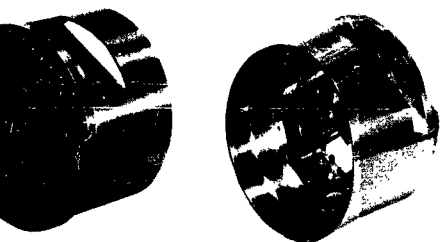
nd, showing,
ace, lock
spacer,
rotor,

End A
L
R

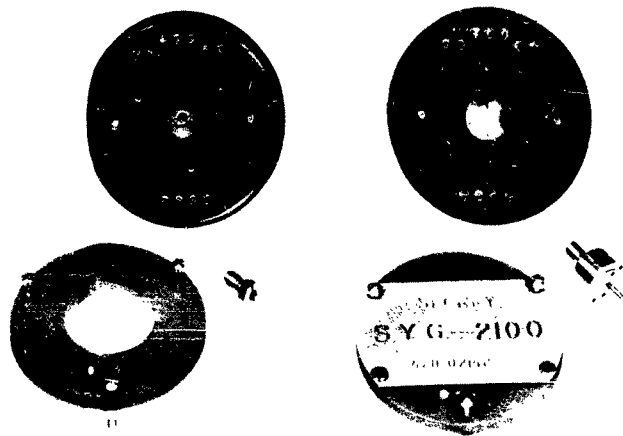


A

4



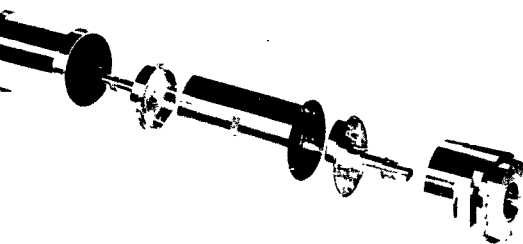
End housings



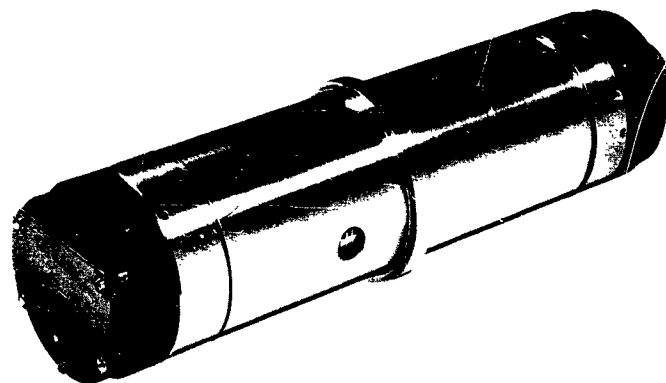
End Assemblies -

Left - Reference Alternator Coupling

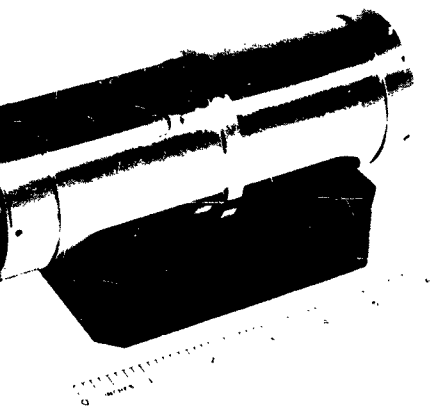
Right - Mercury Grounding Element



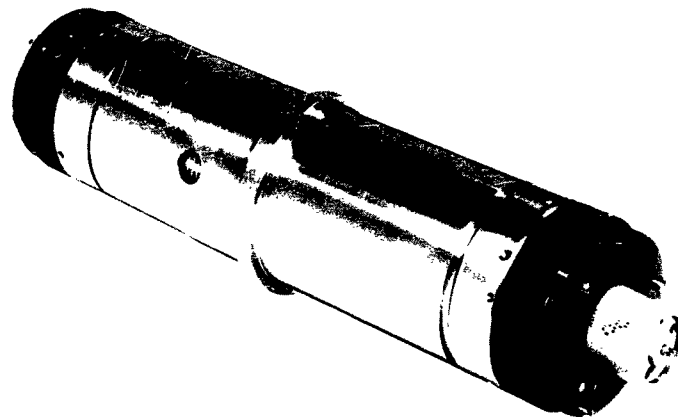
sings, outer case, rotating case and shafts



Assembly - Excitation End



Assembly - End Assemblies Off



Assembly - Signal End

FIGURE 2-8. DETAIL PHOTOGRAPHS

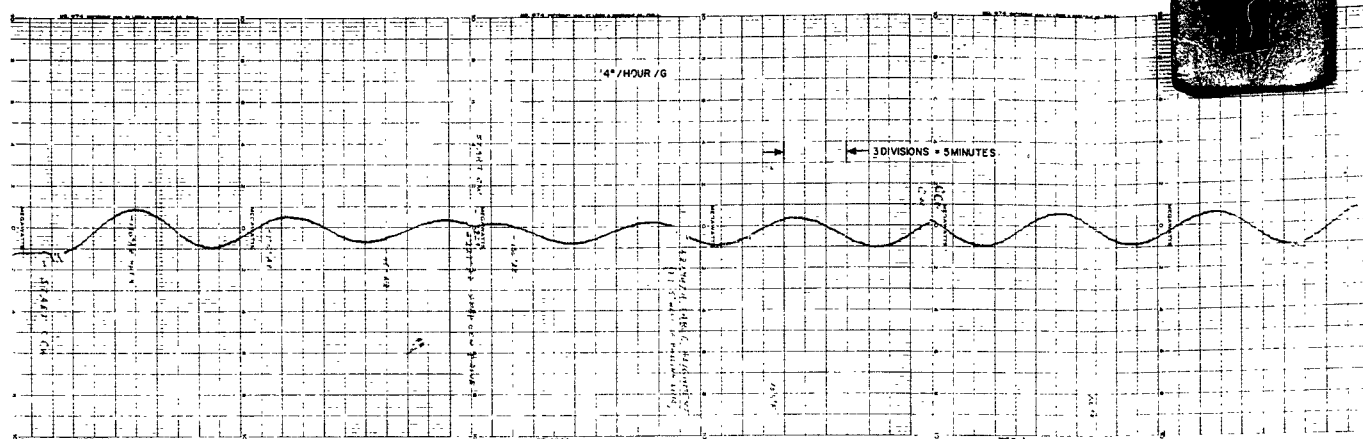
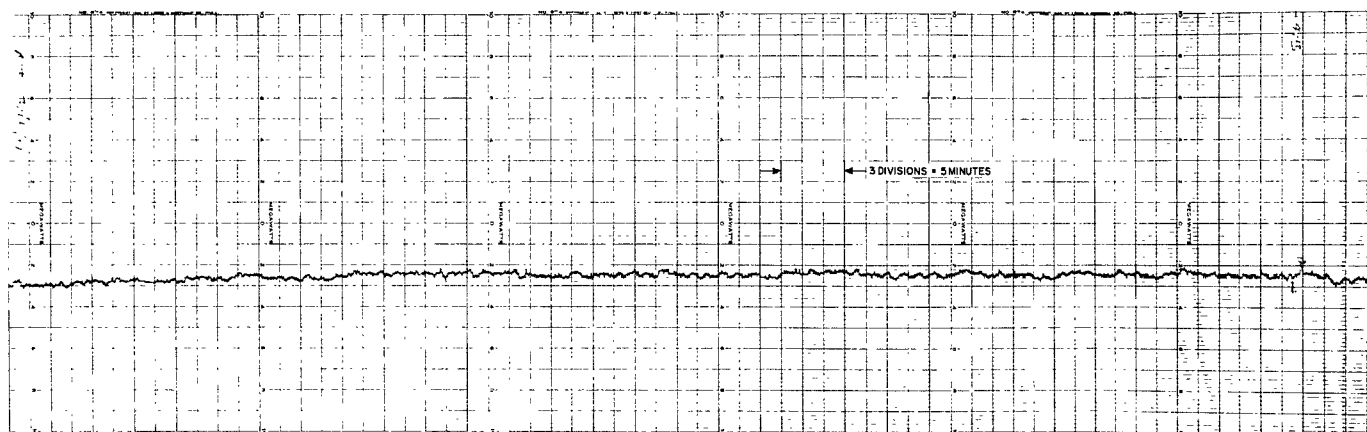
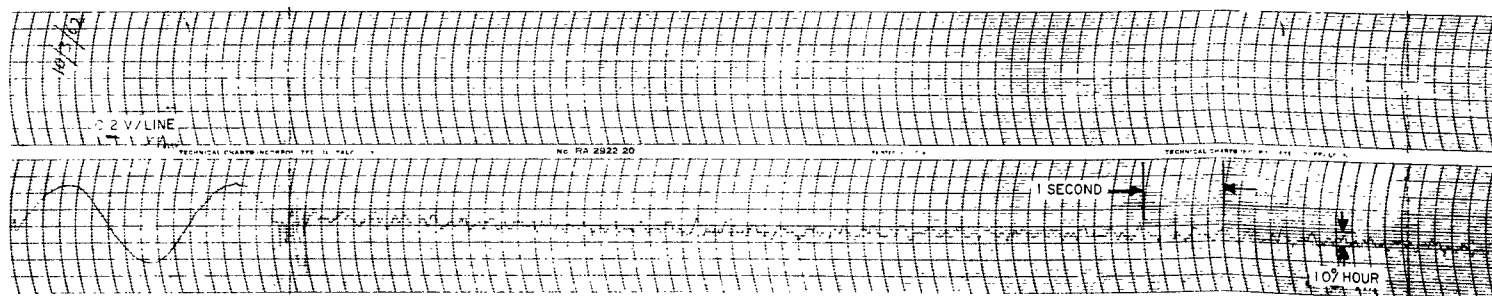


FIGURE 3-4. LIN



FIGURE



2

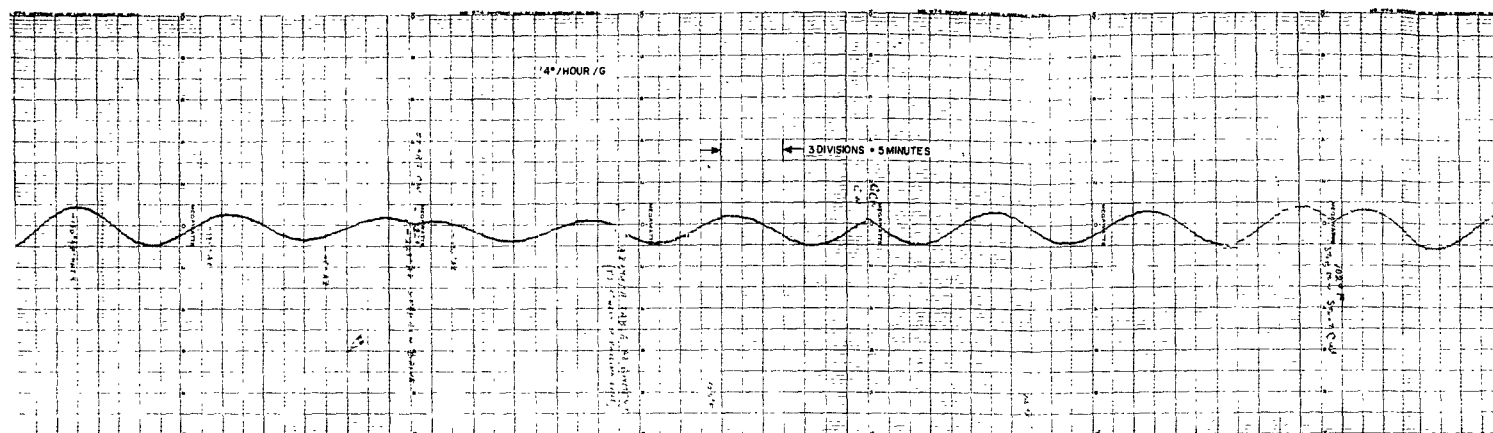


FIGURE 3-4. LINEAR ACCELERATION SENSITIVITY - MODEL II

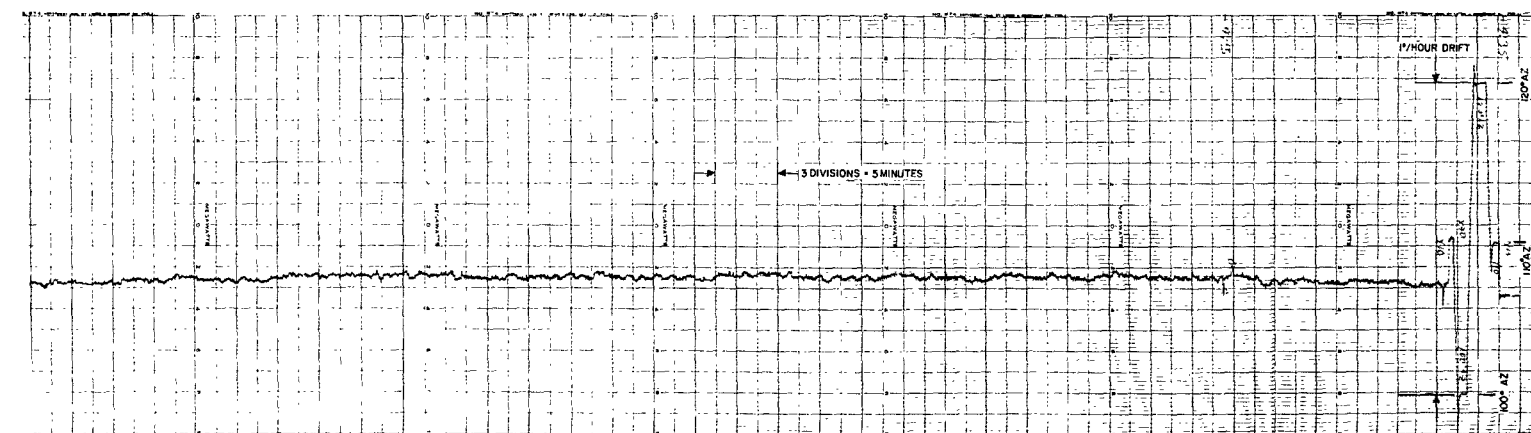


FIGURE 3-5. SENSITIVITY AND DRIFT - MODEL II

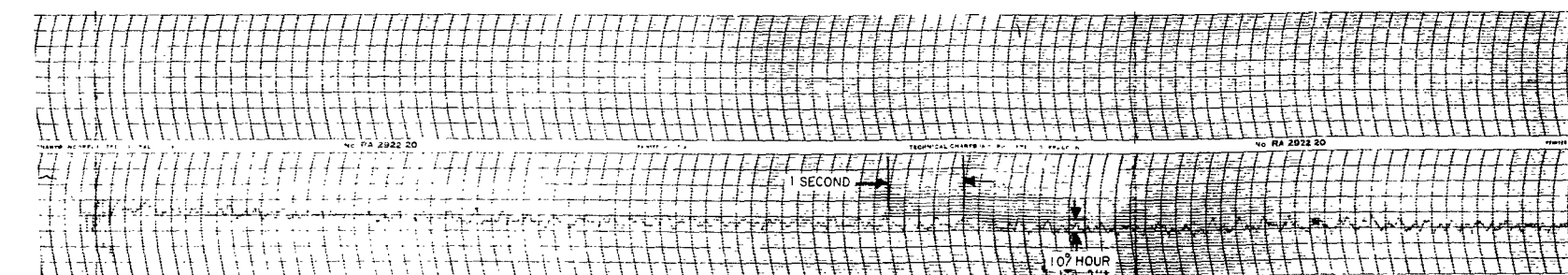


FIGURE 3-6. NOISE - MODEL II

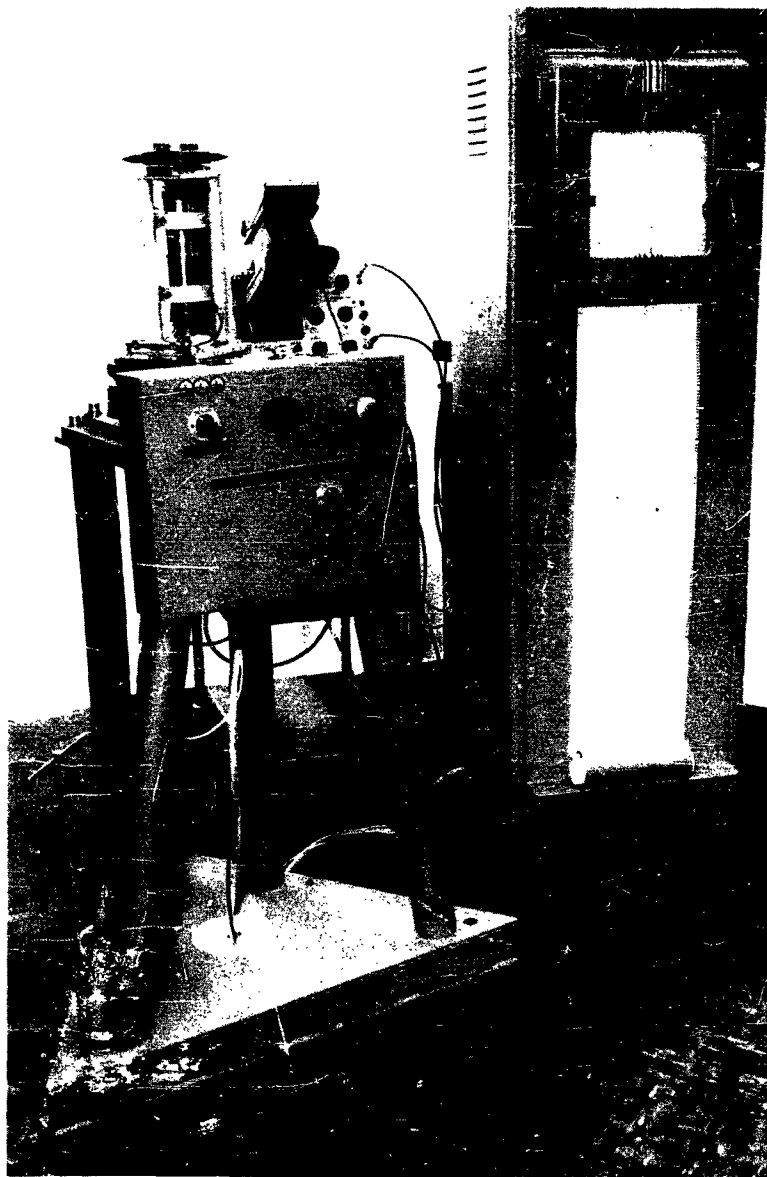


FIGURE 3-7. TYPICAL TEST SET-UP

<p>Aeronautical Systems Division, AF Flight Dynamics Lab, Wright-Patterson AFB, Ohio. Rpt No. ASD-TDR-63-184 DEVELOPMENT PROGRAM FOR AN INERTIAL SENSOR TECHNIQUE. Final report, Jun 63, 46p. incl illus.</p> <p>Unclassified Report</p> <p>This program demonstrated the feasibility of a new gyroscope technique for sensing inertially derived control data. This technique measures centrifugal pressures at the surface of a spinning fluid sphere. These pressures represent displacement of the container axis from that of the fluid and are converted to electrical signals by microphones. The two gyroscope models which were built demonstrated low random drift (0.02°/hr), large linear range (<0.1°/hour to 5°/second with 2% accuracy), short warm-up time (less than 2 minutes),</p> <p>(over)</p>	<p>UNCLASSIFIED</p> <p>1. Gyroscopes 2. Instrumentation 3. Fluid mechanics</p> <p>I. AFSC Project 8222, Task 822209 II. Contract No. AF 33(616)-7756 III. Sperry Gyroscope Co., Div of Sperry Rand Corp., Great Neck, N. Y. IV. CA-4211-0158 V. Not avail fr OTS VI. In ASTIA collection</p>	<p>UNCLASSIFIED</p> <p>1. Gyroscopes 2. Instrumentation 3. Fluid mechanics</p> <p>I. AFSC Project 8222, Task 822209 II. Contract No. AF 33(616)-7756 III. Sperry Gyroscope Co., Div of Sperry Rand Corp., Great Neck, N. Y. IV. CA-4211-0158 V. Not avail fr OTS VI. In ASTIA collection</p>	<p>UNCLASSIFIED</p> <p>1. Gyroscopes 2. Instrumentation 3. Fluid mechanics</p> <p>I. AFSC Project 8222, Task 822209 II. Contract No. AF 33(616)-7756 III. Sperry Gyroscope Co., Div of Sperry Rand Corp., Great Neck, N. Y. IV. CA-4211-0158 V. Not avail fr OTS VI. In ASTIA collection</p>
<p>and design simplicity. They are two-axis gyroscopes.</p> <p>The main problem encountered was sensitivity to cross spin axis linear acceleration which, theoretically, can cause apparent drift if axial thermal gradient is present. The design of the models guarded against inducing thermal gradients but neglected to consider the pressures which could be produced in the fluid by the expansion bellows. This design oversight caused large g-sensitive errors but tests were arranged to observe this error with the bellows caged. The error then was less than 5°/hr/g.</p> <p>In its present state of development this gyroscope is particularly adaptable to strapped down applications where high rates must be accepted without sacrificing low rate performance.</p>	<p>UNCLASSIFIED</p> <p>and design simplicity. They are two-axis gyroscopes.</p> <p>The main problem encountered was sensitivity to cross spin axis linear acceleration which, theoretically, can cause apparent drift if axial thermal gradient is present. The design of the models guarded against inducing thermal gradients but neglected to consider the pressures which could be produced in the fluid by the expansion bellows. This design oversight caused large g-sensitive errors but tests were arranged to observe this error with the bellows caged. The error then was less than 5°/hr/g.</p> <p>In its present state of development this gyroscope is particularly adaptable to strapped down applications where high rates must be accepted without sacrificing low rate performance.</p>	<p>UNCLASSIFIED</p> <p>and design simplicity. They are two-axis gyroscopes.</p> <p>The main problem encountered was sensitivity to cross spin axis linear acceleration which, theoretically, can cause apparent drift if axial thermal gradient is present. The design of the models guarded against inducing thermal gradients but neglected to consider the pressures which could be produced in the fluid by the expansion bellows. This design oversight caused large g-sensitive errors but tests were arranged to observe this error with the bellows caged. The error then was less than 5°/hr/g.</p> <p>In its present state of development this gyroscope is particularly adaptable to strapped down applications where high rates must be accepted without sacrificing low rate performance.</p>	<p>UNCLASSIFIED</p> <p>and design simplicity. They are two-axis gyroscopes.</p> <p>The main problem encountered was sensitivity to cross spin axis linear acceleration which, theoretically, can cause apparent drift if axial thermal gradient is present. The design of the models guarded against inducing thermal gradients but neglected to consider the pressures which could be produced in the fluid by the expansion bellows. This design oversight caused large g-sensitive errors but tests were arranged to observe this error with the bellows caged. The error then was less than 5°/hr/g.</p> <p>In its present state of development this gyroscope is particularly adaptable to strapped down applications where high rates must be accepted without sacrificing low rate performance.</p>

	<p>Aeronautical Systems Division, AF Flight Dynamics Lab, Wright-Patterson AFB, Ohio. Rpt No. ASD-TDR-63-184 DEVELOPMENT PROGRAM FOR AN INERTIAL SENSOR TECHNIQUE. Final report, Jun 63, 46p. incl illus.</p> <p style="text-align: center;">Unclassified Report</p> <p>This program demonstrated the feasibility of a new gyroscope technique for sensing inertially derived control data. This technique measures centrifugal pressures at the surface of a spinning fluid sphere. These pressures represent displacement of the container axis from that of the fluid and are converted to electrical signals by microphones. The two gyroscope models which were built demonstrated low random drift (0.02°/hr), large linear ranges (<0.1°/hour to 5°/second with 2% accuracy), short warm-up time (less than 2 minutes),</p> <p style="text-align: center;">(over)</p>	<p>1. Gyroscopes 2. Instrumentation 3. Fluid mechanics</p> <p>I. AFSC Project 8222, Task 822209 II. Contract No. AF 33(616)-7756 III. Sperry Gyroscope Co., Div of Sperry Rand Corp., Great Neck, N. Y. IV. CA-4211-0158 V. Not avail fr OTS VI. In ASTIA collection</p> <p style="text-align: center;">UNCLASSIFIED</p>
	<p>Aeronautical Systems Division, AF Flight Dynamics Lab, Wright-Patterson AFB, Ohio. Rpt No. ASD-TDR-63-184 DEVELOPMENT PROGRAM FOR AN INERTIAL SENSOR TECHNIQUE. Final report, Jun 63, 46p. incl illus.</p> <p style="text-align: center;">Unclassified Report</p> <p>This program demonstrated the feasibility of a new gyroscope technique for sensing inertially derived control data. This technique measures centrifugal pressures at the surface of a spinning fluid sphere. These pressures represent displacement of the container axis from that of the fluid and are converted to electrical signals by microphones. The two gyroscope models which were built demonstrated low random drift (0.02°/hr), large linear ranges (<0.1°/hour to 5°/second with 2% accuracy), short warm-up time (less than 2 minutes),</p> <p style="text-align: center;">(over)</p>	<p>1. Gyroscopes 2. Instrumentation 3. Fluid mechanics</p> <p>I. AFSC Project 8222, Task 822209 II. Contract No. AF 33(616)-7756 III. Sperry Gyroscope Co., Div of Sperry Rand Corp., Great Neck, N. Y. IV. CA-4211-0158 V. Not avail fr OTS VI. In ASTIA collection</p> <p style="text-align: center;">UNCLASSIFIED</p>
	<p>Aeronautical Systems Division, AF Flight Dynamics Lab, Wright-Patterson AFB, Ohio. Rpt No. ASD-TDR-63-184 DEVELOPMENT PROGRAM FOR AN INERTIAL SENSOR TECHNIQUE. Final report, Jun 63, 46p. incl illus.</p> <p style="text-align: center;">Unclassified Report</p> <p>This program demonstrated the feasibility of a new gyroscope technique for sensing inertially derived control data. This technique measures centrifugal pressures at the surface of a spinning fluid sphere. These pressures represent displacement of the container axis from that of the fluid and are converted to electrical signals by microphones. The two gyroscope models which were built demonstrated low random drift (0.02°/hr), large linear ranges (<0.1°/hour to 5°/second with 2% accuracy), short warm-up time (less than 2 minutes),</p> <p style="text-align: center;">(over)</p>	<p>1. Gyroscopes 2. Instrumentation 3. Fluid mechanics</p> <p>I. AFSC Project 8222, Task 822209 II. Contract No. AF 33(616)-7756 III. Sperry Gyroscope Co., Div of Sperry Rand Corp., Great Neck, N. Y. IV. CA-4211-0158 V. Not avail fr OTS VI. In ASTIA collection</p> <p style="text-align: center;">UNCLASSIFIED</p>
	<p>Aeronautical Systems Division, AF Flight Dynamics Lab, Wright-Patterson AFB, Ohio. Rpt No. ASD-TDR-63-184 DEVELOPMENT PROGRAM FOR AN INERTIAL SENSOR TECHNIQUE. Final report, Jun 63, 46p. incl illus.</p> <p style="text-align: center;">Unclassified Report</p> <p>This program demonstrated the feasibility of a new gyroscope technique for sensing inertially derived control data. This technique measures centrifugal pressures at the surface of a spinning fluid sphere. These pressures represent displacement of the container axis from that of the fluid and are converted to electrical signals by microphones. The two gyroscope models which were built demonstrated low random drift (0.02°/hr), large linear ranges (<0.1°/hour to 5°/second with 2% accuracy), short warm-up time (less than 2 minutes),</p> <p style="text-align: center;">(over)</p>	<p>1. Gyroscopes 2. Instrumentation 3. Fluid mechanics</p> <p>I. AFSC Project 8222, Task 822209 II. Contract No. AF 33(616)-7756 III. Sperry Gyroscope Co., Div of Sperry Rand Corp., Great Neck, N. Y. IV. CA-4211-0158 V. Not avail fr OTS VI. In ASTIA collection</p> <p style="text-align: center;">UNCLASSIFIED</p>